Proceedings of the ASME 2010 3rd Joint US-European Fluids Engineering Summer Meeting and 8th International Conference on Nanochannels, Microchannels, and Minichannels
FEDSM-ICNMM2010
August 1-5, 2010, Montreal, Canada

FEDSM-ICNMM2010-30882

PRESSURE DROP OF ACCELERATING SLUG FLOW IN MICROCHANNELS: MODELING AND EXPERIMENT

Shahnawaz Molla
DBR Technology Center
Edmonton, Alberta, Canada

Dmitry Eskin
DBR Technology Center
Edmonton, Alberta, Canada

Farshid Mostowfi[1]
DBR Technology Center
Edmonton, Alberta, Canada

ABSTRACT

An investigation on the pressure drop of a gas-liquid slug flow through a long microchannel of rectangular cross-section is presented. A constant pressure gradient in the microchannel was observed in a flow where gas bubbles progressively expanded and the flow velocity increased due to significant pressure drop. In contrast to majority of the earlier studies of slug flow in microchannels, where void fraction was nearly constant throughout the channel, we investigated systems where the volume of the gas phase increased significantly due to large pressure drop (up to 2000 kPa) along the lengthy (~1 m) channel. This expansion of the gas phase led to a significant increase in the void fraction, causing considerable increase in flow velocity.

Local pressure was measured along the channel using a series of embedded membranes acting as pressure sensors. The axial pressure profile for a gas-liquid system, namely, Dodecane/Nitrogen was studied. Our investigation on pressure gradient showed linear trend over a wide range of void fractions (30–90%) and flow conditions in the two-phase flow. The lengths and the velocities of the liquid slugs and the gas bubbles were also studied along the microchannel by employing video imaging technique. Furthermore, a model describing the gas-liquid slug flow in long microchannels was developed. Excellent agreement between the developed model and the experimental data was obtained.

INTRODUCTION

Gas-liquid slug flow in microchannels is of great interest in practical applications such as monolith reactor, microelectronic cooling, and micro reaction control. The flow pattern in micro scale is largely dominated by viscous forces and surface tension [1-2]. Controlled production of liquid slugs and gas bubbles based on superficial flow of the two phases has been studied extensively to predict the void fraction, liquid film thickness, and pressure drop in the channel [3-4]. It is necessary to understand the pressure characteristics in the two-phase flow in microchannels to estimate operating conditions in different applications. The pressure drop in gas-liquid flow is commonly estimated by assuming homogenous flow condition or based on Lockhart and Martinelli approach [5-6]. Excellent reviews discussing these models are available in literature [1, 7].

In the Lockhart and Martinelli approach, the pressure is calculated based on the pressure drop pertinent to the single phase flow of either liquid or gas. The ratio of the pressure gradient in liquid-only flow to gas-only flow is defined as Lockhart-Martinelli factor. The single phase pressure drop is multiplied by a frictional multiplier which is calculated as a function of the Lockhart-Martinelli factor. Several correlations have been proposed to estimate the frictional multiplier for laminar and turbulent flow conditions [8]. These correlations have been widely used to explain experimental observations of two-phase flow at relatively large Reynolds numbers ($Re>1000$) and show reasonable agreement with measured pressure drop and void fractions. However, it has been reported that for laminar flows ($Re<100$) in small channels (hydraulic diameter<500μm), the Lockhart and Martinelli approach fails to predict the pressure drop accurately [9-10]. It should be noted that both Lockhart-Martinelli approach and homogeneous model do not take the type of flow regime, such as slug, bubbly, or annular flow, into account.

[1] Corresponding author. Email: fmostowfi@slb.com

Another challenge is to calculate the pressure drop in a lengthy capillary channel where the flow accelerates along the channel due to the increase in gas volume caused by the reduction in pressure. Majority of the earlier studies observed pressure drop in Taylor flow over a short length (~100 mm) of the channel and appropriately assumed the expansion of gas bubbles to be negligible. As a result, the effect of the changing flow velocity was not taken into account [4, 11].

The model developed in this work allows us to accurately predict the pressure drop inside a long microchannel when the gas bubbles expand significantly. The model is validated against experimental data obtained for the gas-liquid slug flow in a serpentine microchannel.

MODEL DEVELOPMENT

The model considers a fully developed gas-liquid slug flow through a long horizontal microchannel of a rectangular cross-section. The gas phase is assumed to have low solubility in the liquid phase. The gas bubbles, separating the liquid slugs, expand with the decreasing pressure along the channel. Due to the large pressure gradient, the expansion of the gas phase can be significant. The model assumes that the gas bubbles, separating the liquid slugs, are sufficiently large to neglect mutual interactions between the slugs. Variations of properties of both phases, such as density and viscosity due to change in pressure, are small in the system investigated and therefore neglected.

Pressure Drop in Two-Phase Flows

The pressure drop in an incompressible flow through a narrow channel is primarily governed by the viscous liquid-wall friction. In a fully developed laminar flow, the pressure gradient necessary for driving the liquid at a specified flow rate can be calculated by using the Hagen-Poiseuille type equation:

$$\frac{\Delta p}{L} = (fRe)\frac{8\mu_L Q}{\pi D_h^{\,4}} = (fRe)\frac{2\mu_L U}{D_h^{\,2}} \tag{1}$$

where, μ_L is the liquid viscosity, Q is the average volumetric flow rate through the channel, and U is the mean flow velocity. For channels of a circular cross section, the hydraulic diameter (D_h) is equal to the channel diameter. In this work, the hydraulic diameter is calculated by assuming a constant rectangular cross section of the channel. The frictional loss is accounted for by the friction factor *fRe* (also known Poiseuille number, *Po*). This friction factor for a channel with rectangular cross section can be estimated using the following correlation [12]:

$$Po = fRe = 24(1 - 1.3553\lambda + 1.9467\lambda^2 - 1.7012\lambda^3 + 0.9564\lambda^4 - 0.2537\lambda^5) \tag{2}$$

where $\lambda = H/W$. H and W are the height and the width of the channel, respectively. *Po* is equal to 16 for circular channels. The minor losses caused by the bends in the channel are negligible.

Let us consider a two-phase flow. Depending on the ratio of the liquid/gas flow rates, the flow pattern in the microchannel varies significantly [7]. In this study, we only consider well defined slug flows. When the flow velocity in the narrow channel is relatively slow (low *Re*), the effect of interfacial tension is considerable. Bretherton developed the theoretical framework for the calculation of the pressure drop across a curved interface of a gas bubble surrounded by a thin liquid film in a channel [13].

We employ an approach, whereby the pressure drop in a slug flow can be calculated as a superposition of the pressure drop along the liquid slugs and the gas bubbles, respectively (*e.g.*, Kreutzer *et al.* [11]). The pressure drop due to the presence of the gas bubbles can be taken into account by modifying the friction factor. Based on experimental and CFD studies of slug flows in capillaries, Kreutzer *et al.* [5] found out that the friction factor in a relatively rapid slug flow can be calculated using the semi-empirical correlation:

$$f_{TP} = \frac{Po}{Re}\left[1 + a\frac{D_h}{L_s}\left(\frac{Re}{Ca}\right)^{1/3}\right] \tag{3}$$

where a is the fitting parameter that is evaluated based on the experimental data, Ca is the capillary number, and L_s is the length of a single liquid slug. Kreutzer *et al.* reported different values of a from 0.07 to 0.17. They showed that the above equation is valid for $Ca \sim O(10^{-2})$.

The first term in the bracket of Eq. (3) represents the frictional loss in the liquid phase, while the second term accounts for the pressure loss in the gas phase. The dimensionless numbers $Re(=D_h\rho_L U_m/\mu_L)$ and $Ca(=U_m\mu_L/\sigma)$ in Eq. (3) represent the inertial and interfacial effects respectively (σ is the interfacial tension). It should be noted that the ratio Re/Ca does not depend on the mixture velocity U_m.

Kreutzer *et al.* [11] demonstrated a successful application of Eq. (3) for calculation of slug flows where the gas-liquid volume ratio was constant. Let us extend this approach to expanding flows in lengthy microchannels. When the thickness of the liquid film surrounding the gas bubbles is considered negligible, the cross-sectional areas of the liquid slugs and gas bubbles are almost equal. This assumption is made based on Bretherton's results for low values of Ca (film thickness is calculated as $\delta_F = 0.66 D_h Ca^{2/3}$). For the range of parameters explored in this work, the film thickness is estimated to be negligible compared to the channel dimensions ($\delta_F/D_h << 10^{-3}$). In this case, the volume fraction of a certain phase in the channel is proportional to the total length of the segments occupied by that phase. The volume fraction of the gas phase (ε) and liquid phase ($1-\varepsilon$) can be written as:

$$\varepsilon = \frac{L_G}{L_S + L_G}$$
$$1 - \varepsilon = \frac{L_S}{L_S + L_G} \tag{4}$$

where L_S and L_G are the length of the liquid slugs and gas bubbles, respectively.

The mixture velocity U_m for a liquid-gas system is calculated as

$$U_m = u_L(1-\varepsilon) + u_G\varepsilon \tag{5}$$

where u_L and u_G are the local velocities of the liquid slug and the adjacent gas bubble, respectively.

Similarly, the total mass flux of the mixture is

$$\dot{M} = \rho_L(1-\varepsilon)u_L + \rho_G \varepsilon u_G \tag{6}$$

where ρ_L and ρ_G are the density of the liquid and the gas phases, respectively ($\rho_G/\rho_L \approx 10^{-2}$). While the volume flow rate increases in the streamwise direction due to reduction in local pressure, the mass flux is constant.

Since the film thickness is negligible, it is possible to assume that the liquid and the gas phases move with the same velocity. Then the local velocity of the liquid slug can be expressed from Eq. (6) as:

$$u_L = \frac{\dot{M}}{\rho_L(1-\varepsilon) + \rho_G\varepsilon} = \frac{\dot{M}}{\rho_L(1-\varepsilon)\left\{1 + \frac{\rho_G}{\rho_L}\frac{\varepsilon}{1-\varepsilon}\right\}} \tag{7}$$

Let us calculate the pressure gradient in the microchannel by Eq. (1). Note, the pressure gradient along the slug and the bubble is different; therefore, the pressure gradient should be calculated as an average for a pair of “slug+bubble”. Substituting Eq. (7) into Eq. (1), we obtain the equation for the pressure gradient distribution along the channel as:

$$\frac{\Delta p}{(L_S + L_G)} = (f_{TP}Re)\frac{2\mu_L}{\rho_L D_h^2}\left[\frac{\dot{M}}{\left\{1 + \frac{\rho_G}{\rho_L}\frac{\varepsilon}{1-\varepsilon}\right\}}\right] \tag{8}$$

Substituting the modified friction factor (Eq. (3)) into Eq. (8) we obtain the final form for the gradient as:

$$\frac{\Delta p}{(L_S + L_G)} = \frac{2\mu_L Po}{\rho_L D_h^2}\left[1 + a\frac{D_h}{L_s}\left(\frac{Re}{Ca}\right)^{1/3}\right]\left[\frac{\dot{M}}{\left\{1 + \frac{\rho_G}{\rho_L}\frac{\varepsilon}{1-\varepsilon}\right\}}\right] \tag{9}$$

Here, we would like to emphasize that the term Re/Ca is independent of velocity and L_s and mass flow rate are constant along the channel. Furthermore, if

$$\frac{\rho_G}{\rho_L}\frac{\varepsilon}{1-\varepsilon} \ll 1 \tag{10}$$

Then the right-hand-side of Eq. (9) is nearly constant, which results in uniform pressure gradient throughout the channel. Though the obtained result appeared as unexpected for an accelerating flow, its validity was confirmed by the experiment. However, the value of the term in Eq. (10) becomes significant (~10%), when void fraction exceeds 95%. As a result, the average pressure gradient calculated using Eq. (9) is no longer constant.

EXPERIMENT

Experimental Setup

A number of experiments have been conducted to analyze the flow pattern and the pressure distribution in the microchannel. A brief description of the experimental setup and corresponding results are presented here. Fig. 1 shows a schematic diagram of the experimental setup. The setup consists of a microfluidic device with a long serpentine channel (~0.8m). The device was comprised of a Silicon substrate, in which the channels were etched using conventional deep reactive ion etch. The top substrate was made of a 1.1mm glass wafer, which was bonded to the Silicon substrate using anodic bonding. The channel in these experiments had a uniform rectangular cross section along the length of the channel (W~117μm, H~58μm, based on SEM measurement). Along the channel, ten equally spaced pressure membranes are embedded. Pressure drop along the channel was measured using the membranes, while a high speed camera recorded the void fraction along the channel. The membranes would deform outward under the local static pressure. The deformation of the membranes was then measured using a confocal chromatic sensor (CCS Optima, STIL, France). The manufacturer of the sensor reported an accuracy of 60nm. The membrane was designed for 1μm deformation per 680kPa pressure. This would result in an accuracy of 40kPa for pressure measurement. Each membrane was calibrated individually using a constant hydrostatic pressure before the tests.

The liquid was injected at high pressure (910-2100kPa) from the sample bottle. Gas was supplied from the gas cylinder at the T-junction located 15mm after the liquid inlet. The exit of the channel was maintained at atmospheric pressure. The flow rate of the liquid and gas was regulated by the pump and the regulator on the cylinder, respectively.

To develop the slug flow during the experiments, the gas was injected at a fixed pressure through the side port and the liquid flow rate was gradually increased until well defined slugs/bubbles were observed throughout the channel. It was difficult to develop discrete slugs when the liquid flow was low, relative to the gas flow. As the gas injection pressure increased, the liquid flow necessary to establish proper slugs also increased. In all experiments, the liquid flow rate was increased until the slug flow was observed all along the channel. The flow was monitored for about 10 minutes prior to every measurement to ensure stable conditions. The pressure measurement and video recording were conducted simultaneously.

Experimental Results

Experiments were conducted to study the pressure drop of slug flow for Dodecane/Nitrogen systems. Dodecane was procured form Sigma Aldrich (USA) and was used as supplied. The physical properties of the liquid used in this study are shown in Table 1. The value of σ is estimated based on similar *n*-alkanes.

Table 1 Physical properties of the liquid used in the experiments at 20°C and atmospheric condition [14].

Liquid	ρ_L (kg/m^3)	μ_L (Pa.s)	σ (N/m)
Dodecane	747	0.0015	0.025

Single Phase Flow: Liquid Only. Each set of experiment was initially conducted with flow of liquid phase only through the channel. The liquid was supplied at a constant flow rate. The pressure measurement along the channel and measured liquid flow rate was used to estimate the friction factor in the channel. The results were compared to the theoretical predictions based on Eq. (1) and (2), as shown in Fig. 2 for Dodecane. The error bars shown in the plot represent standard deviation calculated from three iterations of the experiment under similar conditions. The measurements (shown as symbols) were in good agreement with the theory (solid line) for the single phase flow. The uncertainties related to the measurement of pressure and flow rate in the experiments were not significant. The friction parameter, *fRe*, evaluated based on the single phase flow through the channel was reasonably close (within 5%) to the value calculated using Eq. (2) for the channel dimensions. Owing to the fabrication process involved in creating the microfluidic device, the channel cross section may deviate from rectangular geometry. However, the results shown in Fig. 2 indicate that impact of such irregularity on measured parameters is negligible.

Two-Phase Flow in the Channel. Following the experiment with the liquid-only flow, gas was injected into the channel to create the slug flow. The single phase flows from the sample bottle (Dodecane) and the gas tank (N_2) were manipulated to establish a steady flow of gas bubbles trapped between liquid slugs. The microchip in Fig. 1 shows an actual two-phase flow in the channel during the experiments. It was observed that the volume fraction of the two phases varied in the channel. The measurements were conducted in the middle of the channel to minimize the influence of entrance and exit.
The experimental parameters such as flow rate, injection pressure, and void fraction were varied so that a range of Reynolds numbers from 5 to 25 and for capillary numbers from 0.01 to 0.04 can be explored.

Void fraction in the microchannel. Fig. 3 shows the distribution of the liquid phase volume along the channel for different flow rates of liquid and gas. The horizontal axis shows the normalized axial locations along the channel. The volume fractions along the channel length are measured based on image analysis of the video images recorded during the experiments. The void fractions in the channel are calculated by averaging the gas volume fractions from more than 300 consecutive frames. Similar technique for void fraction measurement has been employed by others [2, 4]. As the pressure decreases in the channel, the gas phase expands and gradually occupies larger volume in the channel. Consequently, the liquid volume fraction decreases along the channel at lower pressure.

Local velocity of liquid slugs. For an incompressible fluid, the velocity remains constant along the channel. However, in two-phase flow through a long channel, the local velocity of the slugs is affected by the local pressure. The velocity measured at various locations along the channel is shown in Fig. 4. The average local velocities of the slugs are also obtained based on image analysis of the recorded videos. The locations, where velocities are measured coincided with the locations of the pressure taps. The results shown in the plot are time averaged velocity of the slugs at each location. It is evident that the velocity of the liquid slugs increases along the channel to maintain the same mass flux in the direction of the flow. The lines in the plot show calculated value of the local velocity for constant mass flow rates and local void fraction. The mass flow rate in each case is estimated based on the velocity and fluid properties at the inlet condition. The local velocity in the channel is calculated by Eq. (7) and shows reasonable agreement with the data for most part of the channel.

Pressure drop in microchannel. The pressure profiles in the microchannel for the two phase flows described above are shown in Fig. 5. The subfigures (Fig. 5a-d) show the variation of the liquid fraction in the channel (slugs appear as grey); arranged in increasing order (a-d) of inlet pressure ($p_{gas,in}$= 910-2000kPa). As can be seen in the figure, the gas volume fraction at the inlet is largest in Fig. 5a and progressively decreases in the Fig. 5b-d. The symbols in the plot represent measured pressure values at the pressure taps in the experiments. The pressure drop in all cases was observed to be fairly linear (R^2>0.95).

Notably, the linear trend was observed consistently in all the experiments with slug flow, over a wide range of gas volume fractions in the channel (ε=0.3-0.9). However, due to the variation of local velocity along the channel, the pressure gradient is expected to be a function of the axial location [15-16]. Hence, the direct measurement of pressure at various locations inside the channel provides important information regarding the pressure distribution in the narrow channel for Taylor flow. In addition, the local slug velocity and the volume fractions of the phases can be related to the pressure drop in the channel. In the next section, the model described earlier is used to predict the pressure profile in the channel under experimental conditions.

COMPARISON WITH MODEL PREDICTION

The simple model described above is used to predict the pressure drop in the channel for a slug flow. The measured values of the gas volume fraction and slug velocity in the experiments are used to calculate the effective friction factor for the two-phase flow. The parameter *a* in Eq. (3) is evaluated by fitting the equation to experimentally measured pressure gradient. The fitting parameter, *a*, calculated in this manner varied slightly along the channel with increasing slug velocity and gas volume fraction. The value of *a* calculated for the flow parameters at the first pressure tap was used in the model to determine the pressure profile in the channel. Depending on the slug lengths measured in the experiments, *a* varied from 0.06 to 0.6.

The pressure profiles obtained from the model are compared against the experimental measurements in the plot in Fig. 5. The lines in the plots represent the model predictions for Dodecane-N_2 flow in the channel. The model predictions are in good agreement with the experimental observation of linear pressure profile in the channel. Interestingly, the constant pressure gradient observed in this study is not supported by the existing models for two-phase flow; *e.g.*, Lockhart-Martinelli and homogeneous model. These models predict the pressure gradient to increase with increasing gas volume fraction. Based on these models, the local pressure drop would be nonlinear under the condition of increasing void fraction in the channel.

Thus, the linear pressure drop predicted by the proposed model agrees well with the experimental data. An increase in frictional pressure drop due to the increase in slug velocity is counterbalanced by a proportional increase in the length of the “bubble+slug” pair, resulting in an almost constant pressure gradient. The model developed also shows (see Eqs. (9) and (10)) that the pressure gradient starts deviating from a constant value significantly, if the gas volume fraction reaches 95%.

CONCLUSION

Pressure distribution of a gas-liquid slug flow along a rectangular cross section microchannel was measured. Constant pressure gradient was observed along the channel for various void fractions. The linear pressure drop observed in the experiments was modeled using a semi-empirical approach. The model predicted the pressure drop by taking into account the variation of void fraction and velocity along the channel. Model predictions agreed well with the experimental observation. The model also shows the limit of the linear pressure drop trend in the context of gas-liquid slug flow in microchannels.

ACKNOWLEDGMENTS

Authors would like to thank Dr. Patrick Tabeling from ESPCI, Paris for his valuable comments. The financial support received by S. Molla from Alberta Ingenuity R&D Associate program is gratefully acknowledged.

NOMENCLATURE

a	=	fitting parameter
Ca	=	Capillary number
D_h	=	hydraulic diameter (m)
f	=	Darcy friction factor
H	=	channel height (m)
L	=	length (m)
L_S,, L_G	=	length of slug and bubble, respectively (m)
$\dot{M}$	=	mass flux (kg/m^2/s)
p	=	pressure (Pa)
Po	=	Poiseuille number
Q	=	flow rate (m^3/s)
Re	=	Reynolds number
U	=	mean flow velocity (m/s)
U_m	=	mixture velocity (m/s)
u_L, u_G	=	local velocity of liquid and gas, respectively
W	=	channel width

Greek Symbols

Δ	=	difference
δ_F	=	film thickness (m)
ε	=	void fraction
λ	=	ratio of height to width of the channel
μ	=	dynamic viscosity (Pa.s)
ρ	=	density (kg/m^3)
σ	=	interfacial tension (N/m)

REFERENCES

[1] Angeli, P., and Gavriilidis, A., 2008, "Hydrodynamics of Taylor Flow in Small Channels: A Review," Proceedings of the Institution of Mechanical Engineers Part C-Journal of Mechanical Engineering Science, 222(5), pp. 737-751.

[2] Chung, P. M. Y., Kawaji, M., Kawahara, A., and Shibata, Y., 2004, "Two-Phase Flow through Square and Circular Microchannels - Effects of Channel Geometry," Journal of Fluids Engineering-Transactions of the ASME, 126(4), pp. 546-552.

[3] Field, B. S., and Hrnjak, P., 2007, "Adiabatic Two-Phase Pressure Drop of Refrigerants in Small Channels," Heat Transfer Engineering, 28(8-9), pp. 704-712.

[4] Kawahara, A., Chung, P. M. Y., and Kawaji, M., 2002, "Investigation of Two-Phase Flow Pattern, Void Fraction and Pressure Drop in a Microchannel," International Journal of Multiphase Flow, 28(9), pp. 1411-1435.

[5] Akbar, M. K., Plummer, D. A., and Ghiaasiaan, S. M., 2003, "On Gas-Liquid Two-Phase Flow Regimes in Microchannels," International Journal of Multiphase Flow, 29(5), pp. 855-865.
[6] Lockhart, R. W., and Martinelli, R. C., 1949, "Proposed Correlation of Data for Isothermal 2-Phase, 2-Component Flow in Pipes," Chemical Engineering Progress, 45(1), pp. 39-48.
[7] Cheng, L. X., Ribatski, G., and Thome, J. R., 2008, "Two-Phase Flow Patterns and Flow-Pattern Maps: Fundamentals and Applications," Applied Mechanics Reviews, 61(5).
[8] Fries, D. M., Trachsel, F., and Von Rohr, P. R., 2008, "Segmented Gas-Liquid Flow Characterization in Rectangular Microchannels," International Journal of Multiphase Flow, 34(12), pp. 1108-1118.
[9] Akbar, M. K., and Ghiaasiaan, S. M., 2006, "Simulation of Taylor Flow in Capillaries Based on the Volume-of-Fluid Technique," Industrial & Engineering Chemistry Research, 45(15), pp. 5396-5403.
[10] Ribatski, G., Wojtan, L., and Thome, J. R., 2006, "An Analysis of Experimental Data and Prediction Methods for Two-Phase Frictional Pressure Drop and Flow Boiling Heat Transfer in Micro-Scale Channels," Experimental Thermal and Fluid Science, 31(1), pp. 1-19.
[11] Kreutzer, M. T., Kapteijn, F., and Moulijn, J. A., 2005, "Inertial and Interfacial Effects on Pressure Drop of Taylor Flow in Capillaries," AIChE, 51(9), pp. 2428-2440.
[12] White, F. M., 2005, Viscous Fluid Flow, Mcgraw Hill
[13] Bretherton, F. P., 1961, "The Motion of Long Bubbles in Tubes," J of Fluid Mechanics, 10(pp. 166-188.
[14] 2010, Crc Handbook of Chemistry and Physics, CRC Press, Boca Raton.
[15] Fuerstman, M. J., Lai, A., Thurlow, M. E., Shevkoplyas, S. S., Stone, H. A., and Whitesides, G. M., 2007, "The Pressure Drop Along Rectangular Microchannels Containing Bubbles," Lab on a Chip, 7(11), pp. 1479-1489.
[16] Warnier, M. J. F., De Croon, M. H. J. M., Rebrov, E. V., and Schouten, J. C., 2010, "Pressure Drop of Gas-Liquid Taylor Flow in Round Micro-Capillaries for Low to Intermediate Reynolds Numbers," Microfluidics and Nanofluidics, 8(1), pp. 33-45.

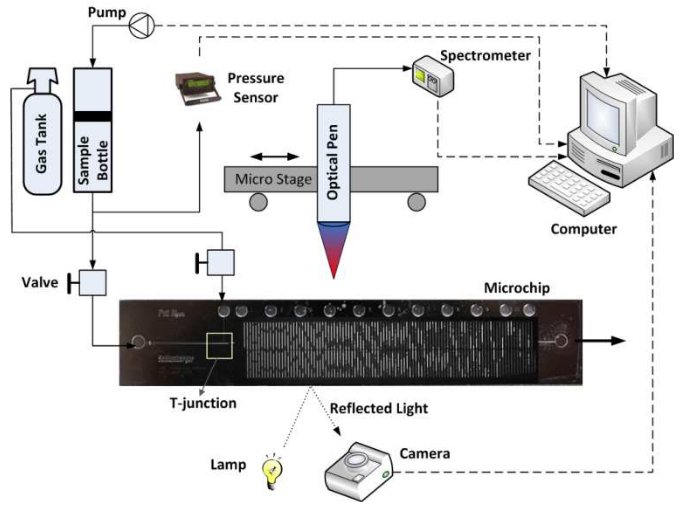

Fig. 1 Schematic of the experimental setup. The microfluidic device is placed in front of a high speed camera. The optical pen (confocal chromatic sensor) was set on a micro-stage to scan the deformation of the membranes used at pressure taps. The fluid is injected from a sample bottle using a high pressure syringe pump. Software developed in-house was used for data acquisition and image analysis.

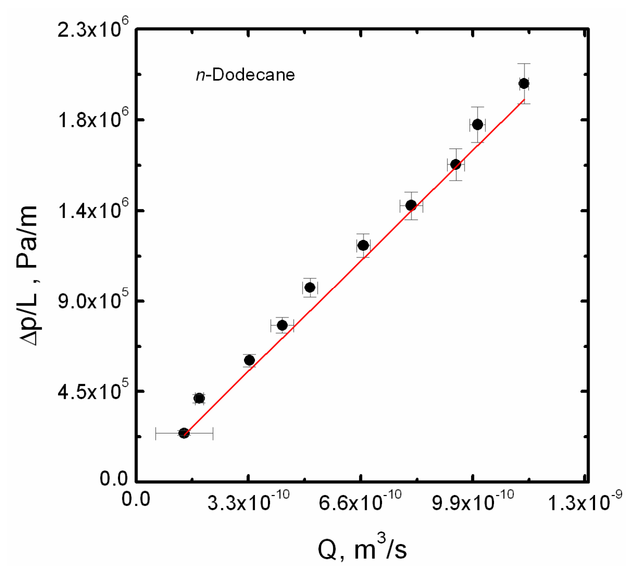

Fig. 2 Correlation between the measured pressure gradient and the flow rate for a single phase liquid (Dodecane) flow. The experimental data (solid circles) is compared with theoretical values (line). The error bars shown in the plot represent standard deviation calculated from three iterations of the experiment under similar conditions. The experiments were conducted at room temperature.

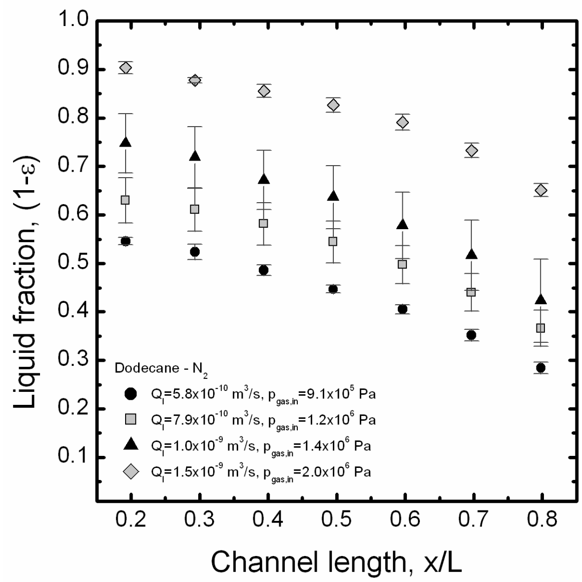

Fig. 3 Liquid phase volume distribution in the capillary for the slug flow. The horizontal axis shows the scaled channel length. The vertical axis shows the liquid volume fraction along the length of the channel. The liquid fraction is shown for the slug flow of Dodecane-N_2 for different liquid and gas flow rate. The experiments were conducted at room temperature.

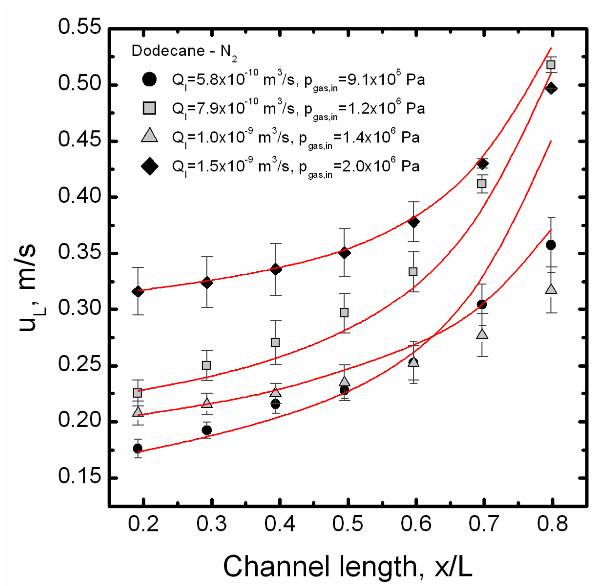

Fig. 4 Average slug velocity under different flow conditions. Time averaged values of velocities at different axial positions were calculated from the experimental videos. The horizontal axis shows the scaled channel length. The slug velocity estimated by Eq. (7) for each case is shown by the solid lines. The error bars shown in the plot represent standard deviations based on image analysis. The experiments were conducted at room temperature.

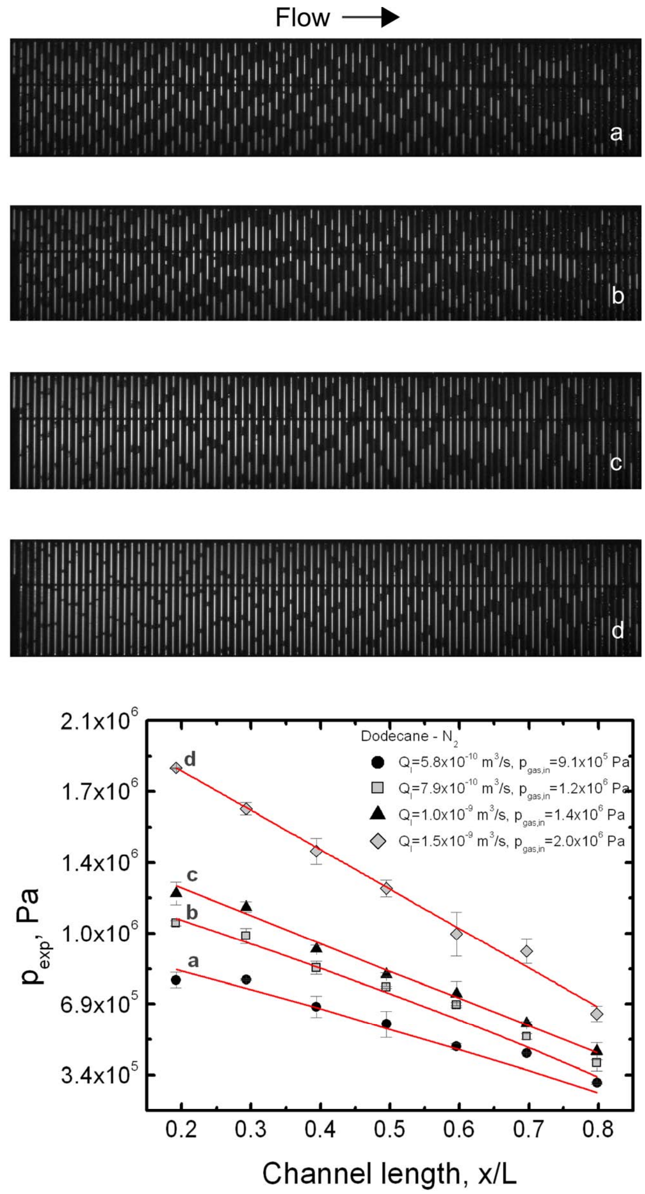

Fig. 5 Snapshots of slug flow under different conditions (increasing liquid fraction, a-d). Comparison of experimental pressure profile with model prediction under similar condition, slug flow of Dodecane/N_2.